Inorg. Chem. **2007**, *46*, 4778–4780

Synthesis, Characterization, and Optical Properties of In_2O_3 Semiconductor Nanowires

Guoxiu Wang,*[†,‡] Jinsoo Park,[‡] David Wexler,[†] Min Sik Park,[‡] and Jung-Ho Ahn[§]

School of Mechanical, Materials and Mechatronic Engineering, Institute for Superconducting and Electronic Materials, University of Wollongong, NSW 2522, Australia, and Department of Materials Engineering, Andong National University, Korea

Received March 1, 2007

In_2O_3 semiconductor nanowires were synthesized by the chemical vapor deposition method through carbon thermal reduction at 900 °C with 95% Ar and 5% O_2 gas flow. The In_2O_3 nanowires were characterized by field emission scanning electron microscopy (FE-SEM), high-resolution transmission electron microscopy (HRTEM), and photoluminescence spectroscopy (PL). For the first time, we observed the formation of corundum-type h-In_2O_3 nanowires and branched In_2O_3 nanowires. The PL spectra of In_2O_3 nanowires show strong visible red emission at 1.85 eV (670 nm) at low temperature, possibly caused by a small amount of oxygen vacancies in the nanowire crystal structure.

Semiconductor nanowires have been extensively investigated as building blocks for nanoscale electronic and optoelectronic devices, with the applications ranging from molecular chemical and biological nanosensors, nanocomputing, and data processing to nanoscale light-emitting diodes.[1,2] On the basis of the bottom-up paradigm for fabricating functional nanoscale devices, controllable synthesis of semiconductor nanowires is especially important. Binary semiconducting oxide nanowires have distinctive optical and electronic properties. A number of semiconductor nanowires, such as Ga_2O_3, Sn_2O, CdO, ZnO, and In_2O_3, have been synthesized by the thermal evaporation method.[3,4] In_2O_3 is a wide band gap transparent semiconductor (direct band gap of 3.55−3.75 eV and indirect band gap of 2.6 eV), which can be widely used in electronic and optoelectronic devices, flat panel displays, gas sensors, and photocatalysis.[5] Indium oxide thin films have been investigated both as electronics and gas sensors. High-performance thin-film transistors (TFTs) using transparent In_2O_3 thin films have demonstrated excellent operating characteristics with large field-effect mobilities, a good drain-source current on/off modulation ratio, and near-zero threshold voltages.[6] In_2O_3 thin films prepared by the sol−gel method have exhibited the capability to detect low levels (several hundred ppb) of nitrogen dioxide in air.[7] Nanobelts of In_2O_3 have been synthesized via evaporation of In_2O_3 crystalline powders at 1400 °C.[3d] Here, we report an efficient technique for synthesizing In_2O_3 nanowires by a carbon thermal reduction method. The crystal structure and optical properties of the as-prepared In_2O_3 nanowires were examined by HRTEM and photoluminescence spectroscopy.

Figure 1a shows the X-ray diffraction patterns of In_2O_3 nanocrystalline powders and the as-grown nanowires. All diffraction lines can be indexed to a cubic structure of the bixbyite Mn_2O_3 (I) type, which belongs to the space group *Ia*3 (206). The lattice parameter of In_2O_3 nanowires was calculated to be $a = 10.115$ Å, which is consistent with the standard value for In_2O_3 powders (JCPDS 06-0416). Comparing the diffraction patterns of In_2O_3 powders and In_2O_3 nanowires, it can be seen that the In_2O_3 nanowires present

* To whom correspondence should be addressed. Email: gwang@uow.edu.au.

[†] School of Mechanical, Materials and Mechatronic Engineering, University of Wallongong.

[‡] Institute for Superconducting and Electronic Materials, University of Wallongong.

[§] Andong National University.

(1) (a) Duan, X. F.; Huang, Y.; Cui, Y.; Wang, J. F.; Lieber, C. M. *Nature* **2001**, *409*, 66. (b) Gudiksen, M. S.; Lauhon, L. J.; M. S.; Wang, J. F.; Smith, D. C.; Lieber, C. M. *Nature* **2002**, *415*, 617. (c) Huang, Y.; Duan, X. F.; Cui, Y.; Lieber, C. M. *Nano Lett.* **2002**, *2*, 101.

(2) (a) Law, M.; Greene, L. E.; Johnson, J. C.; Saykally, R.; Yang, P. D. *Nat. Mater.* **2005**, 4, 455. (b) Huang, M. H.; Mao, S.; Feick, H. N.; Yan, H. Q.; Wu, Y. Y.; Kind, H.; Weber, E.; Russo, R.; Yang, P. D. *Science* **2001**, *292*, 1897. (c) Huang, Y.; Duan, X. F.; Cui, Y.; Lauhon, L. J.; Kim, K. H.; Lieber, C. M. *Science* **2001**, *294*, 1313.

(3) (a) Yang, P.; Lieber, C. M. *Science* **1996**, *273*, 1836. (b)Ying, Z.; Wan, Q.; Cao, H.; Song, Z. T.; Feng, S. L. *Appl. Phys. Lett.* **2005**, *87*, 113108. (c) Park, M. S.; Wang, G. X.; Kang, Y. M.; Wexler, D.; Dou, S. X.; Liu, H. K. *Angew. Chem., Int. Ed.* **2005**, *46*, 750. (d) Pan, Z. W.; Dai, Z. R.; Wang, Z. L. *Science* **2001**, *291*, 1947.

(4) (a) Wu, Y. Y.; Feick, H.; Tran, N.; Weber, E.; Yang, P. D. *Adv. Mater.* **2001**, *13*, 113. (b) Vayssieres, L. *Adv. Mater.* **2003**, *15*, 464. (c) Park, W.; Kim, J. S.; Yi, G. C.; Bae, M. H.; Lee, H. J. *Appl. Phys. Lett.* **2004**, 85, 5052. (d) Peng, X. S.; Meng, G. W.; Zhang, J.; Wang, X. F.; Wang, Y. W.; Wang, C. Z.; Zhang, L. D. *J. Mater. Chem.* **2002**, *12*, 1602.

(5) (a) Cui, J.; Wang, A.; Wang, N. L.; Ni, J.; Lee, P.; Armstrong, N.; Marks, T. J. *Adv. Mater.* **2001**, *13*, 1476. (b) Li, B. X.; Xie, Y.; Jing, M.; Rong, G. X.; Tang, Y. C.; Zhang, G. Z. *Langmuir* **2006**, *22*, 9380. (c) Epifani, M.; Siciliano, P.; Gurlo, A.; Barsan, N.; Weimar, U. *J. Am. Chem. Soc.* **2004**, *126*, 4078.

(6) Wang, L.; Yoon, M. H.; Lu, G.; Yang, Y.; Facchetti, A.; Marks, T. J. *Nat. Mater.* **2006**, *5*, 893.

(7) Gurlo, A.; Ivanovskaya, M.; Bârsa, N.; Schweizer-Berberich, M.; Weimar, U.; Göpel, W.; Diéguez, A. *Sensors Actuators B* **1997**, *44*, 327.

10.1021/ic700386z CCC: $37.00
Published on Web 05/12/2007

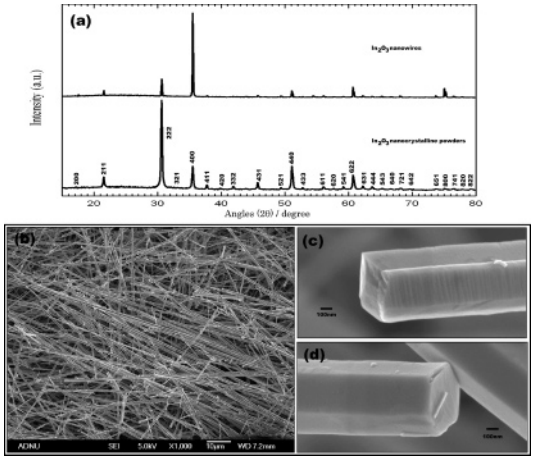

Figure 1. (a) X-ray diffractions of In_2O_3 crystalline powders and as-prepared nanowires. (b) FE-SEM image showing straight In_2O_3 nanowires. (c) FE-SEM image showing the quadrilateral cross-section of a In_2O_3 nanowire. (d) FE-SEM image showing the hexagonal cross-section of a In_2O_3 nanowire.

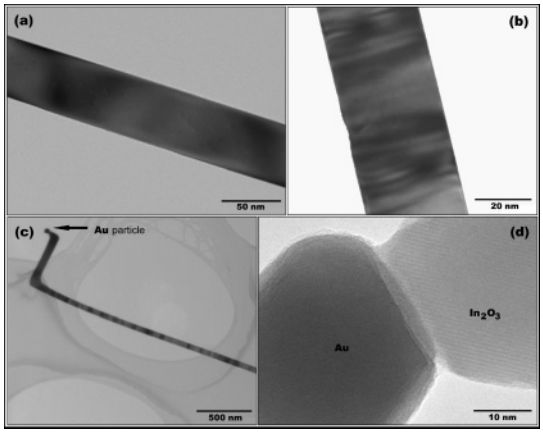

Figure 2. (a) TEM image of a straight In_2O_3 nanowire. (b) TEM image of a ribbonlike In_2O_3 nanowire with bending contour. (c) TEM image of a branched In_2O_3 nanowire with Au nanoparticle at one end. (d) HR-TEM image of the interface of Au−In_2O_3.

their strongest diffraction line at [400] instead of [222] as for In_2O_3 nanopowders. This clearly indicates that the In_2O_3 nanowire lattice grows preferentially along the [010] direction. No impurity phases were identified by X-ray diffraction. After the deposition, we examined the morphology of the white fibrous layer deposited on the surface of the Si substrate by FE-SEM analysis. A general FE-SEM image of the as-grown In_2O_3 nanostructure is shown in Figure 1b. High-density In_2O_3 nanowires had been successfully synthesized. The In_2O_3 nanowires are straight and have a diameter ranging from 30 nm to a few hundred nanometers and a length extending to more than 100 μm. Figure 1c displays the quadrilateral cross-section of an In_2O_3 nanowire with a width- to-thickness ratio of about 1:1. However, we also observed In_2O_3 nanowires with hexagonal cross-sections (as shown in Figure 1d), indicating the corundum-type h-In_2O_3 structure. The preparation of h-In_2O_3 structure requires high temperature and high pressure.[8] Recently, h-In_2O_3 nanocrystals have been synthesized at ambient pressure via surfactant-assisted hydrothermal process.[9] Here, we are able to synthesize h-In_2O_3 nanowires via vapor deposition approach for the first time.

The crystal structure and morphology of individual In_2O_3 nanowires were further characterized by TEM and HRTEM examination. The In_2O_3 fibrous deposits were peeled off the Si wafer via ultrasonic vibration and then dispersed in ethanol to form a suspension. The suspension was then dropped onto a holey carbon grid for TEM analysis. Figure 2a shows a single straight In_2O_3 nanowire with a diameter of about 40 nm. Energy dispersive X-ray analysis (EDX) was performed on the individual In_2O_3 nanowire, revealing that the nanowire consists of only the elements In and O with a ratio of In/O of 41:59, which is close to the In_2O_3 stoichiometry. Figure 2b shows the bending contour under electron diffraction of a ribbonlike In_2O_3 nanostructure with a width of 40 nm. On the basis of a previous report, directly evaporating In_2O_3 at 1400 °C can yield a majority percentage of nanobelts.[3d] Through both SEM and TEM observation, we found that there are 10% nanobelts formed among the deposited In_2O_3 nanowires in our carbon thermal reduction process. Figure 2c shows a branched L-shaped In_2O_3 nanowire with an Au particle at one end. EDX analysis performed at the dark dot confirmed the Au element. The presence of the Au catalyst at the end of nanowires indicated that the growth of In_2O_3 nanowires follows the vapor−liquid−solid (VLS) mechanism. A lattice image of the interface between the Au catalyst and the In_2O_3 nanowire is further shown in Figure 2d, which clearly elucidates the intimate connection between the Au catalyst and the In_2O_3 nanowire. This is the first time that the formation of complex branched L-shaped In_2O_3 nanowires has been reported. It seems that this In_2O_3 nanowire grew along one direction, then suddenly turned 90° and continued to grow perpendicularly to the previous direction. The mechanism governing such complicated growth is unknown. Nevertheless, the synthesis of branched nanowires will be very important for fabricating complex heterostructures and nanoscale devices.

Selected area electron diffraction (SAED) on a single In_2O_3 nanowire demonstrated a single crystalline cubic (bcc) structure (as shown in Figure 3a). The SAED recorded along the [001] zone axis indicated that the In_2O_3 nanowires were growing along the [010] direction. Figure 3b further shows the HRTEM image of an In_2O_3 nanowire. It reveals the lattice fringes of (400) planes, which is perpendicular to the nanowire growth axis [010] direction. We measured the *d* spacing of the In_2O_3 nanowire (400) lattice plane to be 2.50 Å. The presence of Au nanoparticles at the ends of In_2O_3 nanowires directly proves the VLS growth mechanism.[10] In our carbon thermal reduction process, several steps toward the growth of In_2O_3 nanowires may be involved. First, In_2O_3 powders react with carbon, producing In and CO or CO_2. Simultaneously, indium is evaporated and transported by the flowing gas. At a high temperature, when the indium vapor

(8) Prewitt, C. T.; Shannon, R. D.; Rogers, D. B.; Sleight, A. W. *Inorg. Chem.* **1969**, *8*, 1985.
(9) Lee, C. H.; Kim, M.; Kim, T.; Kim, A.; Paek, J.; Lee, J. W.; Choi, S. Y.; Kim, K.; Park, J. B.; Lee, K. *J. Am. Chem. Soc.* **2006**, *128*, 9326.
(10) Li, S. Q.; Liang, X. Y.; Wang, C.; Fu, X. Q.; Wang, T. H. *Appl. Phys. Lett.* **2006**, *88*, 16311.

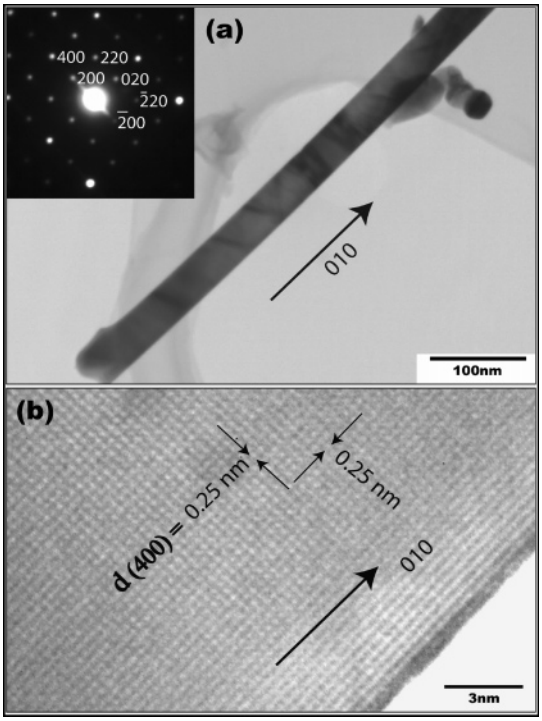

Figure 3. (a) TEM image of a single In_2O_3 nanowire with a diameter of 40 nm. The inset is the SAED recorded along [001] zone axis. (b) HRTEM image of In_2O_3 nanowire lattice.

atoms come into contact with Au on the Si substrate, they form a liquid Au−In eutectic alloy. Because the carrier gas contains 5% O_2 and indium can form a strong covalent bond with oxygen, indium will be oxidized to In_2O_3, resulting in the continuous growth of In_2O_3 nanowires.

The photoluminescence (PL) spectra of the bulk In_2O_3 crystalline powders and the as-deposited In_2O_3 nanowires were measured both at room temperature and at low temperature. The excitation source was a 325 nm He−Cd laser with a power density of 4 mW cm^{-2}. Contrary to the previous reports,[11,12] we did not observe any luminescence at room temperature, either for In_2O_3 powders or for In_2O_3 nanowires. However, we detected a strong red luminescence emission centered at 680 nm for In_2O_3 powders and 670 nm for In_2O_3 nanowires at 10 K, which correspond to 1.80 and 1.85 eV, respectively. The PL spectra of In_2O_3 powders and nanowires are shown in Figure 4. We noticed that the PL emission intensity of In_2O_3 nanowires is almost 10 times of that In_2O_3 powders. It is generally regarded that In_2O_3 is an n-type semiconductor due to oxygen deficiency caused by the various synthetic processes. Although the PL emission mechanism of In_2O_3 is not very clear so far, it has been widely recognized that the oxygen vacancies act as donors and induce PL emission under photon excitation.[13,14] In_2O_3 has an oxygen-deficient fluorite structure with one-fourth of the anions missing in an ordered way.[15] Different synthetic

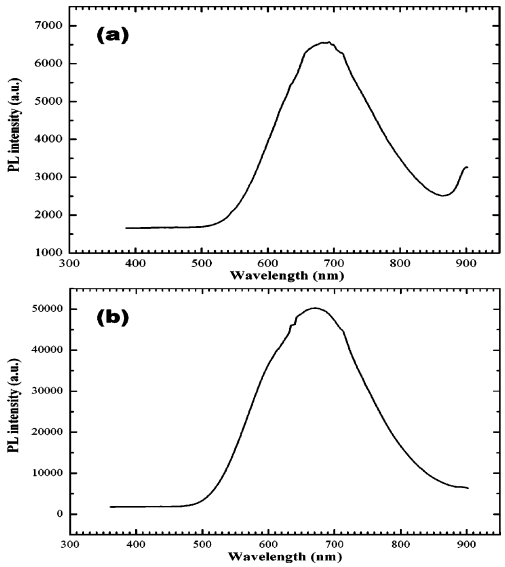

Figure 4. Photoluminescence spectra of (a) In_2O_3 crystalline powders and (b) as-prepared In_2O_3 nanowires. The PL spectra were recorded at 10 K with the laser excitation of 325 nm.

route may lead to varied oxygen vacancies. The lack of PL emission from the as-prepared In_2O_3 nanowires at room temperature indicates that there could be only small amount of oxygen vacancies presented in the In_2O_3 nanowires prepared by CVD process under the oxidizing synthetic atmosphere (5% O_2). The visible red PL emission of In_2O_3 at 10 K is similar to that of In_2O_3 thin films that exhibited orange emission at 637 nm.[16] Since the diameters of In_2O_3 nanowires are much larger than the Bohr radius of In_2O_3 (2.14 nm), quantum-confinement effects can be excluded. Therefore, the observed PL emission could be attributed to a small amount of oxygen vacancies in the In_2O_3 nanowire crystal structure.

In summary, semiconductor In_2O_3 nanowires can be massively synthesized via a carbon thermal reduction process. HRTEM analysis confirmed that the In_2O_3 nanowires grow preferably along the [010] direction and follow the VLS growth mechanism. Complex, branched L-shaped In_2O_3 nanowires were also observed, which could assist in synthesizing branched semiconductor nanowires. We have detected visible red PL emission at low temperature for as-prepared In_2O_3 nanowires.

Acknowledgment. This work was financially supported by the Australian Research Council through the ARC Discovery project (DP0559891). The authors would like to thank Prof. G. C. Yi at Pohang University of Science and Technology (POSTEC), Korea for providing PL measurement.

Supporting Information Available: Details of synthesis of In_2O_3 semiconductor nanowires, XRD, FE-SEM, TEM, HRTEM, and photoluminisence characterizations. This material is available free of charge via the Internet at http://pubs.acs.org.

IC700386Z

(11) Zhou, H.; Cai, W.; Zhang, L. *Appl. Phys. Lett.* **1999**, *75*, 495.
(12) Liu, Q.; Lu, W.; Ma, A.; Tang, J.; Liu, J.; Fang, J. *J. Am. Chem. Soc.* **2005**, *127*, 5276.
(13) Cao, H. Q.; Qiu, X. Q.; Liang, Y.; Zhu, Q. M.; Zhao, M. J. *Appl. Phys. Lett.* **2003**, *83*, 762.
(14) Zheng, M. J.; Zhang, L. D.; Li, G. H.; Zhang, X. Y.; Wang, X. F. *Appl. Phys. Lett.* **2001**, 79, 839.
(15) Liess, M. *Thin Solid Films* **2002**, *410*, 183.
(16) Lee, M. S.; Choi, W. C.; Kim, E. K.; Kim, C. K.; Min, S. K. *Thin Solid Films* **1996**, *279*, 1.